Chemical Science

EDGE ARTICLE

View Article Online
View Journal | View Issue

Cite this: *Chem. Sci.*, 2017, **8**, 5024

Carbon dioxide hydrogenation catalysed by well-defined Mn(I) PNP pincer hydride complexes†

Federica Bertini,[a] Mathias Glatz,[b] Nikolaus Gorgas,[b] Berthold Stöger,[c] Maurizio Peruzzini,[a] Luis F. Veiros,[d] Karl Kirchner*[b] and Luca Gonsalvi*[a]

Received 15th January 2017
Accepted 28th April 2017

DOI: 10.1039/c7sc00209b

rsc.li/chemical-science

The catalytic reduction of carbon dioxide is of great interest for its potential as a hydrogen storage method and to use carbon dioxide as C-1 feedstock. In an effort to replace expensive noble metal-based catalysts with efficient and cheap earth-abundant counterparts, we report the first example of Mn(I)-catalysed hydrogenation of CO_2 to HCOOH. The hydride Mn(I) catalyst [Mn(PNP^{NH}-*i*Pr)(H)(CO)$_2$] showed higher stability and activity than its Fe(II) analogue. TONs up to 10 000 and quantitative yields were obtained after 24 h using DBU as the base at 80 °C and 80 bar total pressure. At catalyst loadings as low as 0.002 mol%, TONs greater than 30 000 could be achieved in the presence of LiOTf as the co-catalyst, which are among the highest activities reported for base-metal catalysed CO_2 hydrogenations to date.

Introduction

Carbon dioxide (CO_2) is the end product of combustion of organic matter and its increasing concentration in the atmosphere is causing great concerns due to its negative effects on the environment. On the other hand, it can represent a cheap, readily available and abundant carbon feedstock, and its utilisation for the production of value-added chemicals and fuels is a hot topic of research today.[1] Among the possible target reactions, the catalytic hydrogenation of CO_2 to formic acid (FA) and its derivatives is a subject of increasing interest, as FA is a widely employed commodity chemical and can be used as a hydrogen storage material.[2]

In recent years, a number of efficient homogeneous catalysts for the hydrogenation of CO_2 to FA under mild reaction conditions have been developed, most of them based on expensive and rare noble metals such as iridium and ruthenium.[3] The replacement of the scarce and expensive noble metals with cheaper, earth abundant, and less toxic first-row transition metals would enhance the sustainability and industrial applicability of these hydrogenation reactions. Recently, iron- and cobalt-based homogeneous catalysts have been reported for this reaction (Scheme 1),[4] and in some cases show a catalytic activity comparable to that observed for some noble metal catalysts. Beller and co-workers described Fe(II)- and Co(II)-PP$_3$ catalysts (PP$_3$ = tripodal tetraphosphines) that could reach significantly high turnover numbers (TONs) for CO_2 hydrogenation to FA and derivatives.[4g,i,j] Milstein reported that the PNP pincer complex *trans*-[Fe(PNP-*t*Bu)(H)$_2$(CO)] promotes the reaction already at a low pressure with TONs up to 788.[4h] In 2015, Hazari, Bernskoetter and co-workers described the catalytic activity of a library of Fe(PNP) pincer complexes exhibiting very high activities which could be even further enhanced using Lewis acid co-catalysts achieving TONs up to *ca.* 59 000. This sets the current state-of-the-art in CO_2 hydrogenation to FA with a non-precious, earth-abundant metal catalyst.[4b] More recently, the beneficial effect of Lewis acid co-catalysts was demonstrated also for related cobalt pincer complexes.[4k]

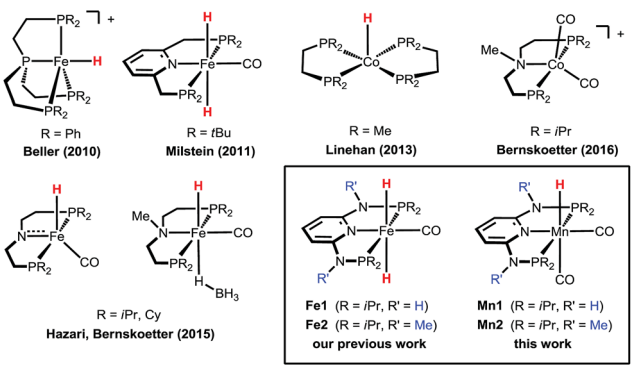

Scheme 1 Examples of efficient base-metal catalysts for the hydrogenation of carbon dioxide to formic acid or formate.

[a]*Consiglio Nazionale delle Ricerche (CNR), Istituto di Chimica dei Composti Organometallici (ICCOM), Via Madonna del Piano 10, 50019 Sesto Fiorentino, Firenze, Italy. E-mail: l.gonsalvi@iccom.cnr.it*

[b]*Institute of Applied Synthetic Chemistry, Vienna University of Technology, Getreidemarkt 9/163-AC, A-1060 Wien, Austria. E-mail: karl.kirchner@tuwien.ac.at*

[c]*Institute of Chemical Technologies and Analytics, ViennaUniversity of Technology, Getreidemarkt 9/163-AC, A-1060 Wien, Austria*

[d]*Centro de Química Estrutural, Instituto Superior Técnico, Universidade de Lisboa, Av. Rovisco Pais No. 1, 1049-001 Lisbon, Portugal*

† Electronic supplementary information (ESI) available: Experimental procedures, NMR and IR spectra, atomic coordinates for DFT optimized structures and computational details, and crystallographic data for **2**. CCDC 1520528. For ESI and crystallographic data in CIF or other electronic format see DOI: 10.1039/c7sc00209b

Recently,[4a] we demonstrated the remarkable catalytic activity of the Fe(II) PNP pincer complexes [Fe(PNP^{NH}-*i*Pr)(H)$_2$(CO)] (**Fe1**) and [Fe(PNP^{NMe}-*i*Pr)(H)$_2$(CO)] (**Fe2**) for CO_2 hydrogenation reaching TONs of up to *ca.* 10 000 in the presence of a base with quantitative yields of formate at 80 °C (Scheme 1). Complex **Fe2** also exhibited a significant activity even at room temperature affording FA in quantitative yield (TON *ca.* 1000) in 24 h. Based on these results, we decided to explore the activities of other earth-abundant metal complexes starting with low valent manganese compounds. As yet, in contrast to iron, manganese plays a minor role, despite the fact that manganese, after iron and titanium, is the third most abundant transition metal in the earth's crust, and ubiquitously available and essentially non-toxic. Reports on homogeneous Mn(I) catalysed reactions only appeared very recently in the literature from the groups of Milstein,[5] Beller,[6] Kirchner,[7] Kempe,[8] and Boncella[9] and their collaborators.

Here, we report the first efficient hydrogenation of CO_2 to FA catalysed by the well-defined Mn(I) catalysts [Mn(PNP^{NH}-*i*Pr)(H)(CO)$_2$] (**Mn1**) and [Mn(PNP^{NMe}-*i*Pr)(H)(CO)$_2$] (**Mn2**). These complexes are isoelectronic with our previously tested Fe(II) catalysts (**Fe1** and **Fe2**), and **Mn1** was shown very recently to be highly active in the dehydrogenative coupling of alcohols and amines to give imines[7a] as well as in the synthesis of substituted quinolines and pyrimidines.[7b]

Results and discussion

The synthesis of the complexes [Mn(PNP^{NH}-*i*Pr)(H)(CO)$_2$] (**Mn1**) and [Mn(PNP^{NMe}-*i*Pr)(H)(CO)$_2$] (**Mn2**) was carried out as recently described by some of us.[7a] In addition, X-ray quality crystals of **Mn2** were grown from toluene/pentane and the corresponding solid state structure was obtained (Fig. 1 and ESI†). The structural data are comparable with those obtained for **Mn1**,[7a] with slightly shorter bond distances for **Mn1**–C20 (1.700 *vs.* 1.747 Å) and longer distances for **Mn1**–C21 (1.784 *vs.* 1.775 Å) and **Mn1**–H1 (1.80 *vs.* 1.46 Å).

Catalytic CO_2 hydrogenation

The catalytic activity of the Mn(I) pincer complexes **Mn1** and **Mn2** was initially tested in a THF/H_2O (10 : 1) solvent mixture in the presence of DBU (DBU = 1,8-diazabicycloundec-7-ene) as the base, at 80 °C, under 80 bar total pressure (H_2 : CO_2 = 1 : 1), for 24 h.[10] Selected results are reported in Table 1. Using a **Mn1**/DBU ratio of 1 : 1000, FA was obtained in quantitative yields with respect to DBU (TON = 1000, entry 1). At lower catalyst loadings (**Mn1**/DBU = 1 : 10 000; [**Mn1**] = 0.18 μmol mL^{-1}), FA was formed in a 55% yield after 24 h (TON = 5520, entry 2). Notably, under such reaction conditions **Mn1** had a superior performance compared to **Fe1** and **Fe2**, which in turn gave the TONs of 2080 and 2750 respectively (entries 3 and 4).

Furthermore, increasing the reaction time for the **Mn1** tests to 48 h significantly improved the yield of formate (86%, TON = 8600, entry 5). In contrast, **Mn2** showed a lower catalytic activity, affording FA in only a 10% yield with a TON of 1010 after 24 h (entry 6). For 3 h runs under standard conditions, **Mn1** gave a TON = 475 (yield = 48%), and **Mn2** gave a TON = 96 (yield = 10%). Decreasing the catalyst concentration to 0.036 μmol mL^{-1} (**Mn1**/DBU = 1 : 50 000) afforded FA in a lower yield (16%) but with a significantly increased TON (9100, entry 11), indicating that the catalyst activity strongly depends on the catalyst/DBU ratio.

The promoting effect of adding H_2O (10%) to THF may be attributed to a water-assisted dissociation of the formate ligand resulting from the CO_2 insertion into the Mn–H bond under catalytic conditions (see DFT calculations), as well as to an improved stabilization of the FA/DBU adduct due to hydrogen bonding. This is supported by the observation that the FA/DBU

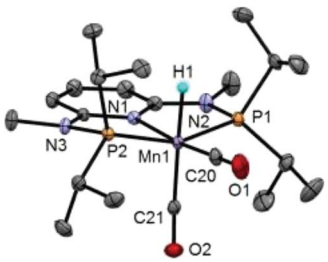

Fig. 1 Structural view of **Mn2** showing 30% thermal ellipsoids (most hydrogen atoms omitted for clarity). Selected bond lengths [Å] and angles [°]: **Mn1**–P1 2.2015(9), **Mn1**–P2 2.1893(9), **Mn1**–N1 2.062(1), **Mn1**–C20 1.700(2), **Mn1**–C21 1.784(2), **Mn1**–H1 1.80(2), P1–**Mn1**–P2 159.28(2), N1–**Mn1**–C20 173.92(7), N1–**Mn1**–C21 95.85(6), C20–**Mn1**–C21 90.23(8).

Table 1 The hydrogenation of CO_2 to FA, catalysed by Mn(I) and Fe(II) complexes in the presence of DBU as the base[a]

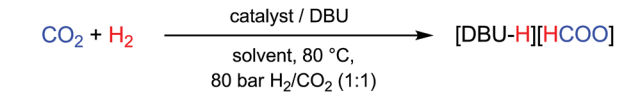

Entry	Cat	Cat/DBU ratio	Solvent	TON[b]	Yield[c] (%)
1	**Mn1**	1 : 1000	THF/H_2O	1000	>99
2	**Mn1**	1 : 10 000	THF/H_2O	5520	55
3	**Fe1**	1 : 10 000	THF/H_2O	2080	21
4	**Fe2**	1 : 10 000	THF/H_2O	2750	28
5[d]	**Mn1**	1 : 10 000	THF/H_2O	8600	86
6	**Mn2**	1 : 10 000	THF/H_2O	1010	10
7	**Mn1**	1 : 10 000	THF	4400	44
8	**Mn2**	1 : 10 000	THF	420	4
9	**Fe1**	1 : 10 000	THF	0	0
10	**Fe2**	1 : 10 000	THF	0	0
11	**Mn1**	1 : 50 000	THF/H_2O	9100	16
12	**Mn1**	1 : 10 000	EtOH	8000	80
13	**Mn2**	1 : 10 000	EtOH	1330	13
14	**Fe1**	1 : 10 000	EtOH	0	0
15	**Fe2**	1 : 10 000	EtOH	10 000	>99
16	**Mn3**	1 : 10 000	THF/H_2O	5750	58

[a] General reaction conditions: catalyst (0.2–10 μmol), 10 mmol DBU, 5.5 mL solvent, 80 °C, 80 bar total pressure (H_2 : CO_2 = 1 : 1), 24 h. [b] TON = (mmol FA)/(mmol catalyst). [c] Yield = [(mmol FA)/(mmol DBU)] × 100. The yield of formate was calculated from the integration of the corresponding ^{1}H NMR signal, using DMF as the standard. [d] 48 h reaction time. All experiments were repeated at least twice, av. error *ca.* 6%.

adduct is immiscible with THF, but cleanly dissolves in H_2O. However, a striking difference between the Mn and Fe catalysts was observed when running the tests in anhydrous THF. Whereas with the Mn(I) complexes FA was formed even in the absence of water, albeit with lower TONs (4400 and 420 for **Mn1** and **Mn2**, entries 7 and 8, respectively), and **Fe1** and **Fe2** were completely inactive under these conditions (entries 9 and 10). We thus re-examined the solvent effects for the Fe catalysts **Fe1** and **Fe2**.[4a]

While their catalytic activity in the THF/H_2O mixtures is comparable (entries 3 and 4), we observed a substantial difference running the tests in EtOH. In this solvent, the catalytic activity of **Fe2** is substantially improved (TON = 10 000; >99% yield, entry 15), while **Fe1** resulted in being totally inactive (0% yield, entry 14), confirming the data previously reported.[4a] The reason for the latter observation is that for **Fe1** EtOH prevents the formation of the key catalytic intermediates [Fe(PNP^{NH}-*i*Pr)(H)$_2$(CO)]. This was not the case for **Fe2**, which readily affords the corresponding dihydrides in the presence of the base and H_2.[11b] We then studied the effect of EtOH in the hydrogenation of CO_2 catalysed by **Mn1** and **Mn2**. To our delight, using EtOH as the solvent improved the catalytic performance of **Mn1** (entry 12) significantly, which afforded FA in an 80% yield (TON = 8000). In turn, only a minor improvement was observed for **Mn2** (entry 13).

Effect of LiOTf

In an effort to further improve the Mn-DBU catalytic system, and in line with literature data on other Fe-pincer systems,[4b] we decided to test the effect of a Lewis acid additive in combination with **Mn1**, choosing LiOTf as it has previously shown to give the highest promoting effect.[4b] The results are summarized in Table 2. As previously observed for **Fe2**,[4a] the addition of LiOTf only had a minor effect on the catalysis in the presence of **Mn1** when the reaction was run in EtOH (entries 1 and 2). In contrast to that, an enhancement effect was observed when using THF/H_2O (10 : 1) as the solvent mixture. At a catalyst concentration of [**Mn1**] = 0.18 μmol mL^{-1} and in the presence of 0.5 mmol of LiOTf (**Mn1**/DBU = 1 : 10 000; **Mn1**/LiOTf = 1 : 1000), FA was obtained in quantitative yields within the first 24 h of the reaction (TON = 10 000, entry 3).

Remarkably, the reaction also proceeds at room temperature, albeit with a TON an order of magnitude lower (TON = 1000, entry 4). Lower catalyst concentrations of 0.036 and 0.018 μmol mL^{-1} resulted in higher TONs but lower yields (entries 5 and 6). A longer catalytic run (entry 7) indicated that the catalyst remains active for up to 48 h, affording FA with a TON = 26 600, a *ca.* two-fold increase compared to the 24 h catalytic run (entry 5), suggesting a constant reaction rate with an average TOF of *ca.* 550 h^{-1}. Increasing the LiOTf amount to 1.0 mmol (**Mn1**/LiOTf = 1 : 5000) resulted in an increased TON = 16 700 (entry 8), whereas a further increase to 1.5 mmol gave a slightly decreased TON = 12 420 (entry 9). As previously suggested,[4b] such an effect may be attributed to the limited LiOTf solubility in such a solvent mixture.

The effect of the temperature on the catalysis was tested by increasing it from 80 to 100 °C, which resulted in a *ca.* 2-fold increase in the TON to 31 600 after 24 h (63% yield, entry 10). However, increasing the temperature further to 115 °C resulted in the formation of an unidentified side product (**4**) in a *ca.* 25% yield with respect to DBU, along with a yield of formate of *ca.* 62% (entry 11). Trace amounts of the same by-product (<5%) were also observed at 100 °C. Careful examination of the ^{1}H and ^{13}C{^{1}H} NMR spectra showed new signals (δ_H = 8.00, δ_C = 161.7) typical for *N*-formyl groups, suggesting that *N*-formylation of DBU occurs as a side reaction at high temperatures (see ESI†). This attribution was confirmed by obtaining the same product independently from the reaction of FA with DBU (1 : 1) at 120 °C

Table 2 CO_2 hydrogenation to FA catalysed by **Mn1** in THF/H_2O (10 : 1) in the presence of LiOTf as the co-catalyst[a]

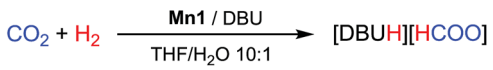

Entry	**Mn1**/DBU ratio	Solvent	LiOTf (mmol)	*T* (°C)	TON[b]	Yield[c] (%)
1	1 : 10 000	EtOH	1.0	80	8700	87
2	1 : 50 000	EtOH	1.0	80	5000	10
3	1 : 10 000	THF/H_2O	0.5	80	10 000	>99
4	1 : 10 000	THF/H_2O	0.5	25	1000	10
5	1 : 50 000	THF/H_2O	0.5	80	13 200	26
6	1 : 100 000	THF/H_2O	0.5	80	14 800	15
7[d]	1 : 50 000	THF/H_2O	0.5	80	26 600	53
8	1 : 50 000	THF/H_2O	1.0	80	16 700	33
9	1 : 50 000	THF/H_2O	1.5	80	12 420	25
10	1 : 50 000	THF/H_2O	1.0	100	31 600	63
11	1 : 50 000	THF/H_2O	1.0	115	31 200	62
12[e]	1 : 50 000	THF/H_2O	1.0	80	30 000	60

[a] General reaction conditions: catalyst (0.1–10 μmol), LiOTf (0.5–1.5 mmol), 10 mmol DBU, 5.5 mL solvent, 80 °C, 80 bar total pressure (H_2 : CO_2 = 1 : 1), 24 h. [b] TON = (mmol FA)/(mmol catalyst). [c] Yield = [(mmol FA)/(mmol DBU)] × 100. The yield of formate was calculated from the integration of the corresponding ^{1}H NMR signal, using DMF as the internal standard. [d] 48 h reaction time. [e] 72 h reaction time. All experiments were repeated at least twice, av. error *ca.* 6%.

in THF/H_2O (10 : 1) in the absence of the catalysts (see details in ESI†). The catalytic tests run at 80 °C with longer reaction times (72 h, entry 12) also gave high TONs of *ca.* 30 000 (60% formate yield) but in this case no *N*-formylation of DBU was observed, confirming that this side reaction is triggered by temperature effects.

Mechanistic studies

Details on the reaction mechanism were obtained for the most active catalytic system, complex **Mn1**, by a combination of experimental NMR techniques and DFT calculations. The reactivity of complexes **Mn1** and **Mn2** towards CO_2 was initially investigated in a stoichiometric reaction by NMR and IR techniques. When a solution of **Mn1** in THF was stirred under an atmosphere of CO_2 (1 bar) for *ca.* 1 min, the immediate formation of the formate complex [Mn(PNP^{NH}-*i*Pr)(CO)$_2$(κ^1-O-OC(O)H)] (**Mn3**) was observed (Scheme 2). The complex precipitated from the solution in essentially quantitative yield (see ESI†). This complex is characterised by a ^{1}H NMR singlet at $\delta = 8.21$ ppm for the proton of the formyl ligand. In the IR spectrum, the characteristic ν_{CO} frequencies for the *cis*-CO and for the formyl carbonyl ligands were observed at 1923, 1842, and 1593 cm^{-1}, respectively. **Mn3** could also be obtained by reacting **Mn1** with 1 equiv. of HCOOH in THF at room temperature. In the case of **Mn2**, no reaction was observed with either CO_2 or HCOOH under the above conditions. It was possible to prove the reversibility of the CO_2 insertion in **Mn1** by reacting **Mn3** with H_2 (70 bar) in the presence of excess DBU at room temperature in THF (Scheme 2), whereas no reaction took place in the absence of base.

Interestingly, isolated **Mn3** was also active in the catalysis, giving comparable activity to **Mn1** under the same test conditions (Table 1, entry 16 *vs.* 2), as expected for a reaction intermediate. The reactivity of **Mn1** with CO_2 to give the formate complexes is somewhat remarkable, since the isostructural and isoelectronic cationic Fe analogues *cis*-[Fe(PNP^{NR}-*i*Pr)(CO)$_2$H]$^+$ (**Fe3**, R = H and **Fe4**, R = Me) were found to be catalytically inactive for the hydrogenation of ketones and aldehydes,[11b] as well as in stoichiometric reactions with CO_2. We reasoned that this could be related to the electron density around the metal and in particular with the M–H bond. Indeed, the corresponding atomic charges (NPA, see ESI†) were found to be $C_{Mn} = -0.92/C_H = -0.13$ in **Mn1** and $C_{Fe} = -0.53/C_H = -0.04$ in **Fe3**, showing an electron richer metallic centre and hydride ligand in the case of **Mn1** (Scheme 3). Moreover, the M–H bond is weaker in the case of M = Mn as shown by the corresponding Wiberg indices[12] ($WI_{Mn-H} = 0.43$, $WI_{Fe-H} = 0.47$), indicating a more reactive hydride for **Mn1** than for **Fe3**. The free energy balances (gas phase) calculated for the reaction of the CO_2 insertion into the M–H bond (Scheme 3) corroborate the previous conclusions, including the absence of the reactivity of **Mn2** toward CO_2 at room temperature.

A deeper insight into the reaction mechanism was obtained by DFT calculations.[13] Free energy profiles obtained for the entire reaction are presented in the ESI.† An explicit water molecule was considered in the model providing H-bond stabilisation for the intermediates (see ESI†). Two alternative mechanisms were investigated for the most active Mn catalyst **Mn1**. In the first mechanism (Scheme 4, left and Fig. S9 in ESI†), a purely metal-centred mechanism is considered, *i.e. without* the participation of the N–H bond of the PNP ligand. This path starts with a nucleophilic attack of the hydride in intermediate **A** to the carbon dioxide C-atom, in an outer sphere reaction. This affords an intermediate (**B**) with a formate ligand bound to Mn in a C–H σ-complex, with an accessible barrier of 9.6 kcal mol^{-1}.[14] **B** is less stable than the initial reactants (**A**) by $\Delta G = 5.2$ kcal mol^{-1}. From **B**, two pathways are possible. Formato ligand isomerisation can be achieved through a transition state with the energy of 13.2 kcal mol^{-1}, yielding a κ^1-O formate complex (**C**, corresponding to isolated **Mn3**), 9.7 kcal mol^{-1} more stable than the reagents, representing a resting state of the catalyst. Alternatively, the exchange of the formate in **B** by one H_2 molecule can give a dihydrogen complex (**F′**), 7.0 kcal mol^{-1} less stable than the initial reagents (**A**). The H_2 coordination step has the highest energy transition state of the entire mechanism ($\Delta G^{\neq} = 17.9$ kcal mol^{-1}). Finally, the deprotonation of the dihydrogen intermediate **F′** (by either formate or DBU) regenerates the initial hydride complex **Mn1** while the final product is obtained as [DBUH][HCOO]. Overall, the reaction has a barrier of 27.6 kcal mol^{-1}, considering **C** as the catalyst resting state, and the entire reaction is thermodynamically favorable with $\Delta G = -11.2$ kcal mol^{-1}.

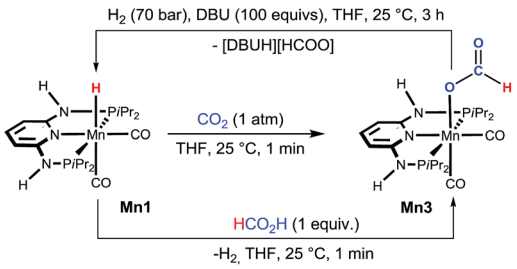

Scheme 2 Reaction of **Mn1** with CO_2 (1 atm) and FA (1 equiv.) to give **Mn3**. For the former reaction, the reversibility from **Mn3** to **Mn1** was also demonstrated.

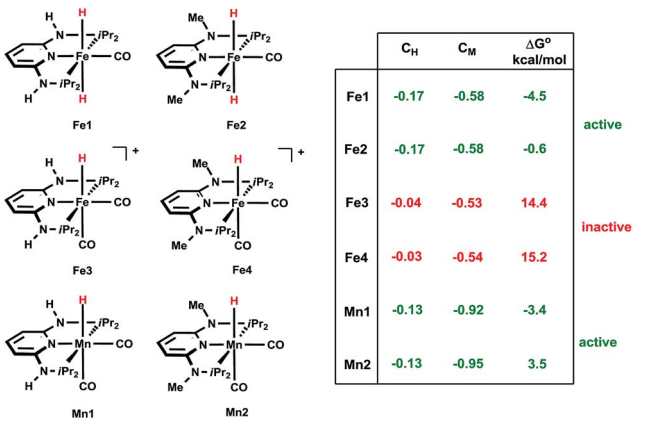

Scheme 3 Comparison of NPA charges for the Fe(II) and Mn(I) pincer complexes and computational free energies ΔG° for the CO_2 insertion into the metal–H bond to yield the κ^1-O formate complexes according to Scheme 2.

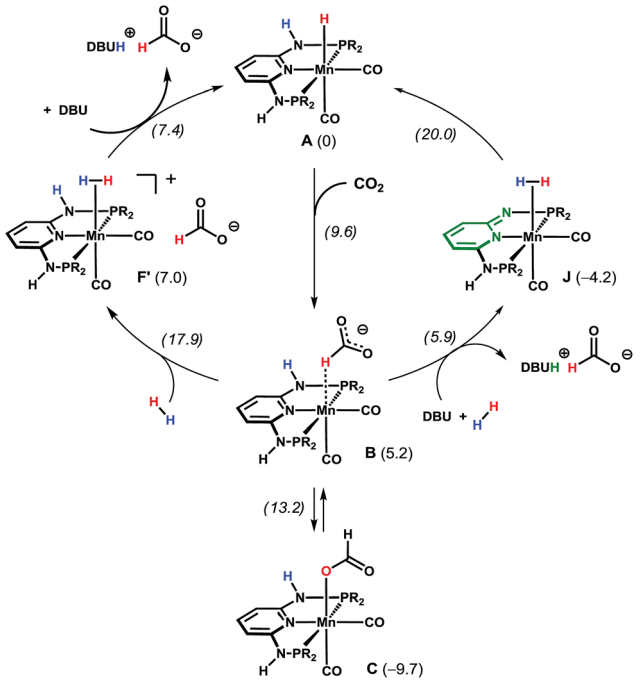

Scheme 4 Simplified catalytic cycles for CO_2 hydrogenation in the presence of **A** (the free energy values in kcal mol^{-1} are with respect to **A**, and the transition state energies are in italics). R = *i*Pr.

In the second path investigated (Scheme 4, right and Fig. S10 in ESI†) a bifunctional mechanism *with* the participation of the N–H bond of the PNP ligand is considered. Here, the first step corresponds to the formation of the Mn-bound formate C–H σ-complex **B**, as in the previous mechanism. From **B**, the base (DBU) deprotonates the N–H group of the PNP ligand and releases the formate ion yielding the product as [DBUH][HCOO]. In turn, the so-obtained five-coordinated Mn neutral complex, bearing a formally negative PNP ligand (Fig. S10 in ESI†), readily coordinates to H_2 and the resulting Mn(η^2-H_2) complex (**J**) is 4.2 kcal mol^{-1} more stable than the starting species **A**. Water- (or protic solvent) assisted H–H bond splitting from complex **J** follows, yielding back the initial catalyst by forming a Mn–H hydride bond and reprotonating the PNP ligand. This last step has a transition as high as 20.0 kcal mol^{-1}, which is the highest of this path. The overall barrier for the reaction is 29.7 kcal mol^{-1} (with respect to **C**), which is within 2 kcal mol^{-1} from the first pathway considered.

We then turned our attention to the effects of the Li additive. We investigated the relative stabilities of the intermediates **B** and **C** in the presence of the $Li(THF)_2^+$ adducts (Fig. 2 and ESI†) and compared them with the values obtained in the absence of Li. The energy difference between **B·Li(THF)$_2$** and **C·Li(THF)$_2$** is 11.2 kcal mol^{-1}, *i.e.*, 3.4 kcal mol^{-1} smaller than the difference between **B** and **C**. The increased stabilisation in **B·Li(THF)$_2$** may be attributed to the κ^2-O,O formate chelation of $Li(THF)_2^+$, and will have a promoting effect on the catalysis by favoring the κ^1-H formate **B** over the κ^1-O formate resting state **C**. To the best of our knowledge, this is the first quantification of the Li effect for base-metal catalysed CO_2 hydrogenation by DFT calculations.

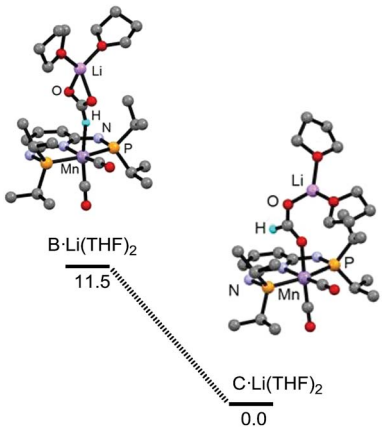

Fig. 2 Relative stability (free energy, kcal mol^{-1}) and structures of the intermediates **B·Li(THF)$_2$** and **C·Li(THF)$_2$**.

In summary, both mechanisms described above are competitive with overall barriers within 2 kcal mol^{-1} of each other. The two pathways feature different roles of the free base (DBU). In the first case, DBU can either react with FA produced from the CO_2 hydrogenation yielding [DBUH][HCOO] in an acid–base process, or deprotonate the η^2-H_2 coordinated ligand, directly forming [DBUH][HCOO]. In the second mechanism, DBU deprotonates the N–H bond of the PNP ligand and forms [DBUH][HCOO] with an uncoordinated formate anion. Based on the results of the catalytic experiments, however, we conclude that the bifunctional pathway must have a major role in the CO_2 hydrogenation in the presence of **Mn1**. In fact, the activity of **Mn2**, whose PNP structure does not allow for metal–ligand cooperation due to the NMe groups instead of NH groups, is much lower than that of **Mn1**.

Conclusions

In conclusion, this study has shown for the first time that CO_2 catalytic hydrogenation to FA can be achieved with high TONs and yields using well-defined hydrido carbonyl Mn(I) PNP pincer complexes in the presence of an added base (DBU) and a Lewis acid (LiOTf), paving the way for the use of manganese as an earth-abundant and cheap metal for efficient Carbon Dioxide Utilization (CDU). DFT calculations showed that, in the case of the most active catalyst **Mn1**, the reaction can follow two competing routes, involving either a metal-centred or a ligand-assisted mechanism, based on the possible bifunctional role of the PNPNR ligand when R = H. Further studies are in progress to assess the effects of ligand structural modifications on this reaction and to expand the scope of the catalysts to other challenging CDU processes.

Acknowledgements

Financial contributions by the ECRF through the project ENERGYLAB are gratefully acknowledged. This work was also supported by COST Action CM1205 CARISMA (Catalytic Routines for Small Molecule Activation). LFV acknowledges Fundação para a Ciência e Tecnologia, grant UID/QUI/00100/

2013. NG and KK gratefully acknowledge the Financial support by the Austrian Science Fund (FWF) (Project No. P29584-N28).

Notes and references

1 (*a*) M. Aresta, A. Dibenedetto and E. Quaranta, *J. Catal.*, 2016, **343**, 2–45; (*b*) I. Omae, *Coord. Chem. Rev.*, 2012, **256**, 1384–1405; (*c*) T. Sakakura, J.-C. Choi and H. Yasuda, *Chem. Rev.*, 2007, **107**, 2365–2387; (*d*) M. Aresta, in *Carbon Dioxide as Chemical Feedstock*, ed. M. Aresta, Wiley-VCH, Weinheim, 2010, pp. 1–13; (*e*) W.-H. Wang, Y. Himeda, J. T. Muckerman, G. F. Manbeck and E. Fujita, *Chem. Rev.*, 2015, **115**, 12936–12973; (*f*) T. Zell and R. Langer, *Recyclable Catalysis*, 2015, **2**, 87–109.

2 (*a*) A. K. Singh, S. Singh and A. Kumar, *Catal. Sci. Technol.*, 2016, **6**, 12–40; (*b*) D. Mellmann, P. Sponholz, H. Junge and M. Beller, *Chem. Soc. Rev.*, 2016, **45**, 3954–3988; (*c*) F. Joo, *ChemSusChem*, 2008, **1**, 805–808; (*d*) S. Enthaler, J. von Langermann and T. Schmidt, *Energy Environ. Sci.*, 2010, **3**, 1207–1217; (*e*) B. Loges, A. Boddien, F. Gärtner, H. Junge and M. Beller, *Top. Catal.*, 2010, **53**, 902–914; (*f*) J. Klankermayer, S. Wesselbaum, K. Beydoun and W. Leitner, *Angew. Chem., Int. Ed.*, 2016, **55**, 7296–7343 (and references therein).

3 (*a*) R. Tanaka, M. Yamashita and K. Nozaki, *J. Am. Chem. Soc.*, 2009, **131**, 14168–14169; (*b*) T. J. Schmeier, G. E. Dobereiner, R. H. Crabtree and N. Hazari, *J. Am. Chem. Soc.*, 2011, **133**, 9274–9277; (*c*) S. Moret, P. J. Dyson and G. Laurenczy, *Nat. Commun.*, 2014, **5**, 1–7; (*d*) J. F. Hull, Y. Himeda, W.-H. Wang, B. Hashiguchi, R. Periana, D. J. Szalda, J. T. Muckerman and E. Fujita, *Nat. Chem.*, 2012, **4**, 383–388; (*e*) A. Boddien, C. Federsel, P. Sponholz, D. Mellmann, R. Jackstell, H. Junge, G. Laurenczy and M. Beller, *Energy Environ. Sci.*, 2012, **5**, 8907–8911; (*f*) G. A. Filonenko, M. P. Conley, C. Copéret, M. Lutz, E. J. M. Hensen and E. A. Pidko, *ACS Catal.*, 2013, **3**, 2522–2526; (*g*) C. A. Huff and M. S. Sanford, *ACS Catal.*, 2013, **3**, 2412–2416; (*h*) K. Muller, Y. Sun and W. R. Thiel, *ChemCatChem*, 2013, **5**, 1340–1343; (*i*) G. A. Filonenko, R. Van Putten, E. N. Schulpen, E. J. M. Hensen and E. A. Pidko, *ChemCatChem*, 2014, **6**, 1526–1530; (*j*) S. F. Hsu, S. Rommel, P. Eversfield, K. Muller, E. Klemm, W. R. Thiel and B. Plietker, *Angew. Chem., Int. Ed.*, 2014, **53**, 7074–7078.

4 (*a*) F. Bertini, N. Gorgas, B. Stöger, M. Peruzzini, L. F. Veiros, K. Kirchner and L. Gonsalvi, *ACS Catal.*, 2016, **6**, 2889–2893; (*b*) Y. Zhang, A. D. MacIntosh, J. L. Wong, E. A. Bielinski, P. G. Williard, B. Q. Mercado, N. Hazari and W. H. Bernskoetter, *Chem. Sci.*, 2015, **6**, 4291–4299; (*c*) O. Rivada-Wheelaghan, A. Dauth, G. Leitus, Y. Diskin-Posner and D. Milstein, *Inorg. Chem.*, 2015, **54**, 4526–4538; (*d*) F. Zhu, L. Zhu-Ge, G. Yang and S. Zhou, *ChemSusChem*, 2015, **8**, 609–612; (*e*) H. Fong and J. C. Peters, *Inorg. Chem.*, 2015, **54**, 5124–5135; (*f*) M. S. Jeletic, M. T. Mock, A. M. Appel and J. C. Linehan, *J. Am. Chem. Soc.*, 2013, **135**, 11533–11536; (*g*) C. Ziebart, C. Federsel, P. Anbarasan, W. Baumann, A. Spannenberg, M. Beller and R. Jackstell, *J. Am. Chem. Soc.*, 2012, **134**, 20701–20704; (*h*) R. Langer, Y. Diskin-Posner, G. Leitus, L. J. W. Shimon, Y. Ben-David and D. Milstein, *Angew. Chem., Int. Ed.*, 2011, **50**, 9948–9952; (*i*) C. Federsel, A. Boddien, R. Jackstell, R. Jennerjahn, P. J. Dyson, R. Scopelliti, G. Laurency and M. Beller, *Angew. Chem., Int. Ed.*, 2010, **49**, 9777–9780; (*j*) C. Federsel, C. Ziebart, R. Jackstell, W. Baumann and M. Beller, *Chem.–Eur. J.*, 2012, **18**, 72–75; (*k*) A. Z. Spentzos, C. L. Barnes and W. H. Bernskoetter, *Inorg. Chem.*, 2016, **55**, 8225–8233.

5 A. Mukherjee, A. Nerush, G. Leitus, L. J. W. Shimon, Y. Ben-David, N. A. E. Jalapa and D. Milstein, *J. Am. Chem. Soc.*, 2016, **138**, 4298–4301.

6 (*a*) S. Elangovan, C. Topf, S. Fischer, H. Jiao, A. Spannenberg, W. Baumann, R. Ludwig, K. Junge and M. Beller, *J. Am. Chem. Soc.*, 2016, **138**, 8809–8814; (*b*) M. Perez, S. Elangovan, A. Spannenberg, K. Junge and M. Beller, *ChemSusChem*, 2017, **10**, 83–86; (*c*) S. Elangovan, J. Neumann, J.-B. Sortais, K. Junge, C. Darcel and M. Beller, *Nat. Commun.*, 2016, **7**, 12641; (*d*) S. Elangovan, M. Garbe, H. Jiao, A. Spannenberg, K. Junge and M. Beller, *Angew. Chem., Int. Ed.*, 2016, **128**, 15590–15594.

7 (*a*) M. Mastalir, M. Glatz, N. Gorgas, B. Stöger, E. Pittenauer, G. Allmaier, L. F. Veiros and K. Kirchner, *Chem.–Eur. J.*, 2016, **22**, 12316–12320; (*b*) M. Mastalir, M. Glatz, E. Pittenauer, G. Allmaier and K. Kirchner, *J. Am. Chem. Soc.*, 2016, **138**, 15543–15546.

8 (*a*) F. Kallmeier, T. Irrgang, T. Dietel and R. Kempe, *Angew. Chem., Int. Ed.*, 2016, **55**, 11806–11809; (*b*) N. Deibl and R. Kempe, *Angew. Chem., Int. Ed.*, 2017, **56**, 1663–1666 (and references therein).

9 A. M. Tondreau and J. M. Boncella, *Organometallics*, 2016, **35**, 2049–2052.

10 As the hydrogenation of CO_2 to FA is a mildly endergonic process, it requires the use of an added base to drive the reaction. Based on our previous work with Fe,[4a] and screening of base effects in other Fe(PNP) systems,[4b] we selected DBU as the base of choice for promoting FA production.

11 (*a*) N. Gorgas, B. Stöger, L. F. Veiros and K. Kirchner, *ACS Catal.*, 2016, **6**, 2664–2672; (*b*) N. Gorgas, B. Stöger, E. Pittenauer, G. Allmaier, L. F. Veiros and K. Kirchner, *Organometallics*, 2014, **33**, 6905–6914; (*c*) B. Bichler, C. Holzhacker, B. Stöger, M. Puchberger, L. F. Veiros and K. Kirchner, *Organometallics*, 2013, **32**, 4114–4121.

12 Wiberg indices are electronic parameters related to the electron density between atoms. They can be obtained from a natural population analysis and provide an indication of the bond strength. See K. B. Wiberg, *Tetrahedron*, 1968, **24**, 1083.

13 (*a*) R. G. Parr and W. Yang, *Density Functional Theory of Atoms and Molecules*, Oxford University Press, New York, 1989; (*b*) Calculations performed at the PBE0/(SDD, 6-31G**) level using the Gaussian 09 package. All calculations included solvent effects (THF) using the PCM/SMD model. A full account of the computational details and a complete list of references are provided in ESI.†

14 All free energy values are relative to the initial reagent **Mn1**.